A setup for efficient frequency tripling of high-power femtosecond laser pulses.

Master's Thesis
by
Henrik Enqvist

Lund Reports on Atomic Physics, LRAP-330
Lund, October 2004

Abstract:

Frequency conversion of lasers is a useful technique to reach a wide range of wavelengths, for example in the UV-region. The majority of ultrafast lasers operate in the infrared region, but by using frequency upconversion they can be made to deliver short UV pulses.

In this Master Thesis frequency conversion of a Ti:Sapphire chirped pulse amplified laser is performed. The third harmonic is generated using two methods. The first is to use the nonlinear properties of air by tightly focusing the beam. The second is to use nonlinear crystals together with a birefringent group velocity compensation plate.
A permanent setup is built and installed at MaxLab beamline D611 to be used in conjunction with a UV and X-ray sensitive streak camera in Time Resolved X-ray Diffraction (TXRD) experiments.

1 Introduction

The majority of ultrafast lasers operate in the infrared region. Ti:sapphire lasers for instance operate around 800 nm. With the use of mode-locking and chirped pulse amplification they can deliver very short pulses with extreme peak powers.
At MaxLab beamline D611 such a laser is used to perform time resolved pump-probe experiments where a sample is excited by the laser and then probed with x-rays. The experimental setup is described in detail in reference [1].

The main application is to make the pump laser beam visible to the X-ray detection system. The x-rays are detected by an ultrafast streak camera. When averaging the images from a number of shots, the synchronization between the laser and the camera has to be very precise or else the time resolution will suffer. In reality there will always be some jitter between the two. However if the camera can see the laser directly, the synchronization will not be so critical since every single-shot image will have a spot showing at which time the laser pulse arrived.

Another application for frequency doubling and tripling is that it can be used to excite more sample materials. With just the wavelength region around 800 nm available, only sample materials which absorb in that particular region can be excited.
If the laser is efficiently frequency doubled or tripled, it can be used to excite samples at shorter wavelengths. This opens up the opportunity to study for instance wide band gap semiconductors or insulators.

The goal of this Master Thesis was to build a compact and easy to use frequency tripler with good conversion efficiency.

2 Nonlinear optics

Nonlinear effects are always present when light propagates through all kinds of materials. Normally the electric fields are far too weak to make the effects noticeable. But if the field strength is high enough the nonlinear response of some materials can be very large. Some engineered crystals, like Potassium Dihydrogen Phosphate and Beta Barium Borate, have both strong nonlinearity and high damage threshold. Their full names are rarely used; instead they are referred to as KDP and BBO.

When exposed to an electric field the material is polarized. This polarization of the material can be expanded into a Taylor series.

$$P(t) = \chi^{(1)}E(t) + \chi^{(2)}E^2(t) + \chi^{(3)}E^3(t) + \ldots \tag{2.1}$$

The first term is the normal linear response of the material. But with higher field strengths the other terms will also be large enough to make a contribution. Of these the second order term will usually be dominant.

The simplest possible nonlinear process is second harmonic generation, often abbreviated SHG. Here photons with frequency ω are merged two and two to produce new photons with frequency 2ω. This is actually just a special case of sum frequency generation, where photons of frequency ω_1 and ω_2 are merged into new photons with frequency ω_3. Sum frequency generation is the product of quadratic nonlinearities in the material. To be exact it comes from the second order term in the Taylor expansion of the nonlinear polarization. In order for this process to be efficient the phase matching condition has to be fulfilled.

$$\vec{k}_1 + \vec{k}_2 = \vec{k}_3 \tag{2.2}$$

So the sum of the wave vectors must be conserved. This is the same as saying that the momentum has to be conserved. The vector notation can be removed since all the processes described here are collinear, meaning that all the wave vectors are parallel. For the special case of second harmonic generation this can be rewritten and simplified. Here the pump beam has index 1 and the harmonic 2.

$$2k_1 = k_2 \quad \Rightarrow \quad 2\frac{n_1\omega}{c} = \frac{n_2 2\omega}{c} \quad \Rightarrow \quad n_1 = n_2 \tag{2.3}$$

So for second harmonic generation the refractive index has to be the same for the fundamental and the harmonic. Normally this is not the case, since the refractive index almost always increases with decreasing wavelength. The solution is to use a birefringent material like BBO or KDP. These have different refractive indices depending on the polarization of the incident light. The refractive index in a polarization direction perpendicular to the optical axis of the crystal is fixed at n_o which is not angle dependant. This is called the ordinary wave. But light that travels though with the other polarization is called the extraordinary wave. In this direction the refractive index is dependant on the crystal cutting angle and is determined by the index ellipsoid.

$$\frac{1}{n(\theta)^2} = \left(\frac{\cos^2\theta}{n_o^2} + \frac{\sin^2\theta}{n_e^2} \right)^{-1} \tag{2.4}$$

Then by selecting the correct cutting angle of the crystal, the phase matching condition can be conserved. This is known as type 1 phase matching. The laser used in this project has a center wavelength of 780 nm. So the wavelength of the second harmonic will be 390 nm. The following curve shows the different refractive indices for the two wavelengths at different cutting angles.

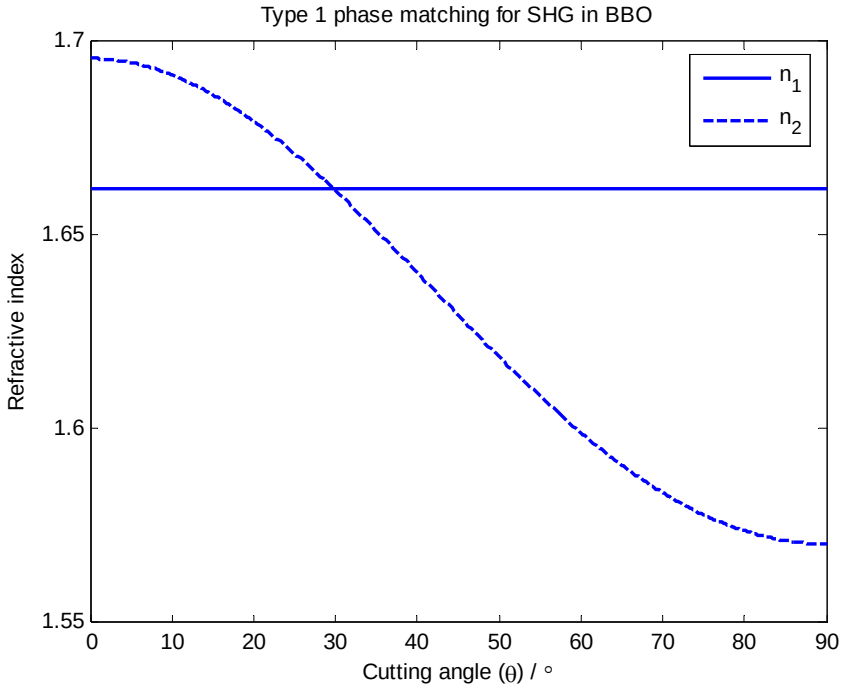

Figure 2.1

The two curves intersect at 30 degrees. So this it the proper cutting angle for this application.

Third harmonic generation, or THG, is then simply sum frequency generation with $\omega_1 = \omega$, $\omega_2 = 2\omega$ and $\omega_3 = 3\omega$. Again using type 1 phase matching, meaning that both the pump beams have ordinary polarization, and the generated harmonic has extraordinary polarization. The phase matching condition (2.2) then reduces to:

$$n_1 + 2n_2 = 3n_3 \tag{2.5}$$

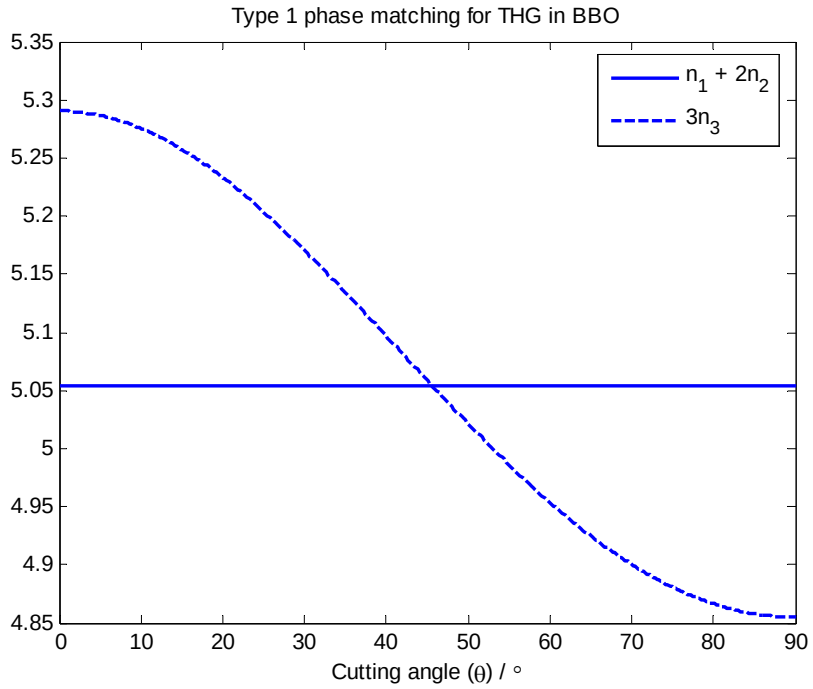

Figure 2.2

The curves here intersect at 45 degrees giving the correct cutting angle for the crystal.

So far the pump beams have had ordinary polarization and the generated harmonic extraordinary. This is referred to as type 1 phase matching. But there is another possibility, which is to let one of the pump beams have extraordinary polarization. This is known as type 2 phase matching. If this is used for second harmonic generation the phase matching condition becomes:

$$n_1 + n_2 = 2n_3 \tag{2.6}$$

Here n_1 and n_2 are the refractive indices for the fundamental in the ordinary and the extraordinary polarization, and n_3 the refractive index for the second harmonic in the extraordinary polarization.

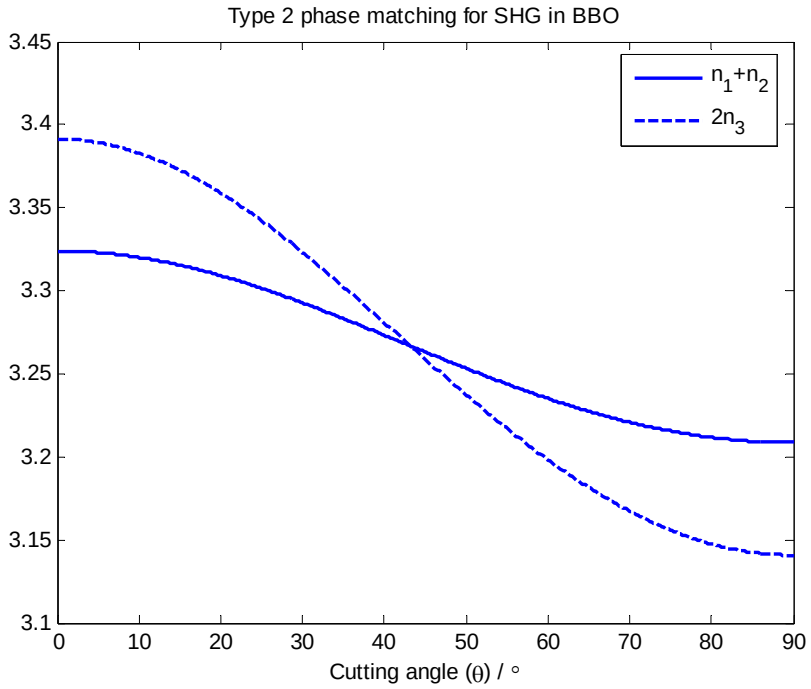

Figure 2.3

The curves intersect at about 43 degrees, which means that it should be possible to use a THG-crystal if it is mounted a bit tilted.

3 Different approaches

3.1 SHG + sum frequency

The most widely used method for third harmonic generation is to use a two step process where the first step is to generate the second harmonic, and then generate the third harmonic by sum-frequency generation of the fundamental and the second harmonic.

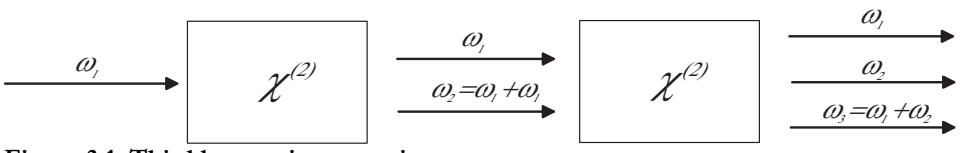

Figure 3.1: Third harmonic generation.

The first step is then to generate the second harmonic. This can for instance be done by using a BBO or KDP crystal cut for type 1 phase matching at the appropriate wavelength.

When using type 1 phase matching for the THG, the polarization of the fundamental and second harmonic should be in the same direction. After SHG, the fundamental and second harmonic are polarized perpendicular to each other. This can anyway be used to generate the third harmonic in a setup like this:

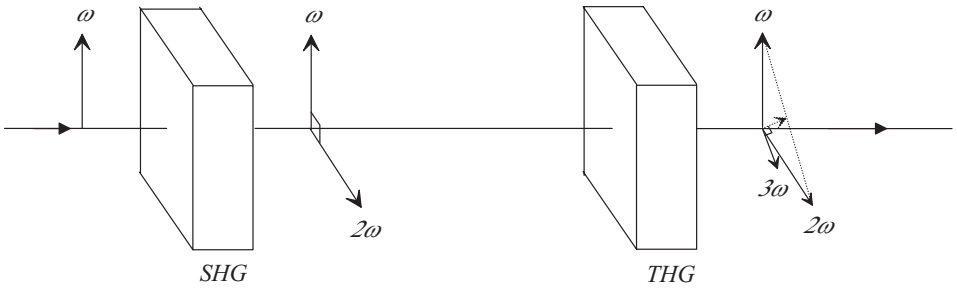

Figure 3.2: Simple setup for THG.

This setup works very well and is easy to align. The previous setup in the lab used this layout. However the efficiency is limited by several things. The

most obvious one is that the polarizations are wrong. And the group velocity difference makes the temporal overlap in the THG crystal less than perfect. This is covered in section 3.1.2.

It is also possible to use type 2 phase matching for the second harmonic generation. The setup would then look like this.

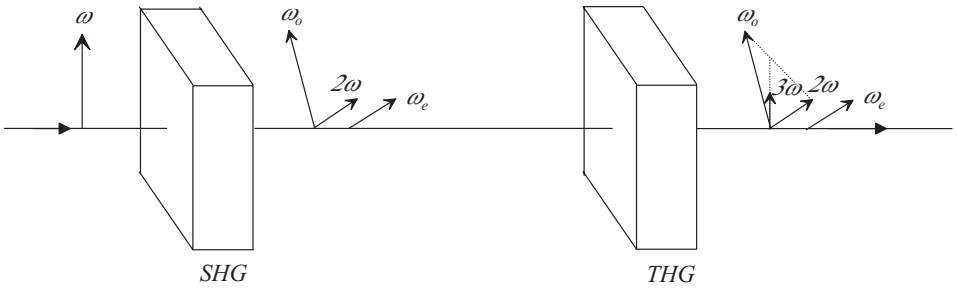

Figure 3.3: Simple THG with type 2 SHG.

Due to the higher group velocity for the extraordinary part of the fundamental, the two polarization directions of the fundamental will separate rather quickly. And since the second harmonic will only be generated in the overlap between the two, that will limit the conversion efficiency. If a thin crystal is used the ordinary part of the fundamental and the second harmonic will still overlap when they exit the crystal, but the extraordinary part of the fundamental will be ahead. Thus in the next crystal the third harmonic is generated only by the overlap of the ordinary part of the fundamental, and the second harmonic. So only half of the pump beam energy is part of the third harmonic generation which of course will limit the conversion efficiency.

Nonlinear crystals are often mounted in protective housings, meaning that the crystal is mounted between thin glass windows. These windows then add a time delay for the second harmonic and thus the fundamental and second harmonic won't overlap in the THG crystal. So for this setup to work both the crystals have to be openly mounted. These very thin crystals may also be grown on a glass substrate. This however is not a problem if the crystals are turned so that the nonlinear materials face each other. Then there will be no glass between the actual crystals.

3.1.1 Correcting the polarization

The setup in figure 3.2 can be improved by inserting a half wave plate between the two nonlinear crystals. The plate should be chosen so that it is a half wave plate for the fundamental. This can then be used to rotate the polarization of the fundamental to any desired angle. The wavelength of the second harmonic is obviously one half of that of the fundamental. This means that if the plate is a half wave plate for the fundamental, it will be a full wave plate for the second harmonic. So while the polarization of the fundamental is changed, the second harmonic is unaffected since full wave plates do not affect the polarization. A setup could for instance look like this:

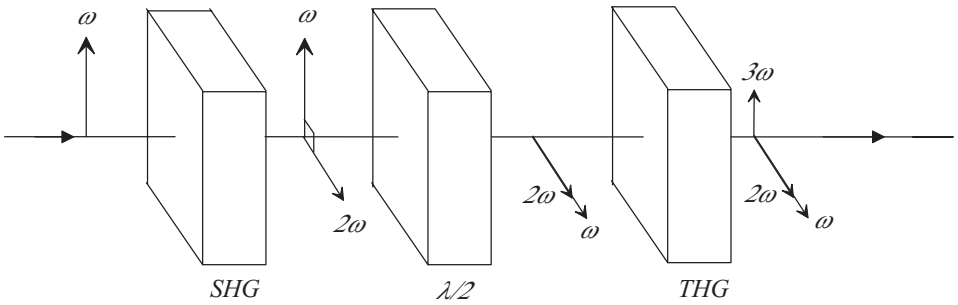

Figure 3.4: THG with half wave plate to correct the polarization.

This setup will work fine for long pulse durations. However, when using pulses in the femtosecond-range this setup will not work at all. This is because the group velocity difference between the fundamental and second harmonic in the half wave plate introduces a delay between the two that is much longer than the pulse duration itself.

3.1.2 The group velocity dispersion

The general formula for group velocity is:

$$v_g = v_p\left(1+\frac{\lambda}{n}\frac{dn}{d\lambda}\right) \tag{3.1}$$

Here v_p is the phase velocity, given by:

$$v_p = \frac{c}{n} \tag{3.2}$$

It is then trivial to calculate the time needed for a pulse to pass a material of length L:

$$t = \frac{L}{v_g} \tag{3.3}$$

Half wave plate

The largest contribution to the total delay comes from the half wave plate. This is commonly made of quartz. There are no reliable data for quartz since the exact composition of the material varies. However it is very similar to fused silica, so instead the data for fused silica is used as an approximation. The refractive index as a function of wavelength is then approximately given by:

$$n^2 = A_0 + A_1\lambda^2 + A_2\lambda^{-2} + A_3\lambda^{-4} + A_4\lambda^{-6} + A_5\lambda^{-8} \tag{3.4}$$

The coefficients can be found in the product catalogs from most manufacturers. For simplicity they are included in Appendix B.

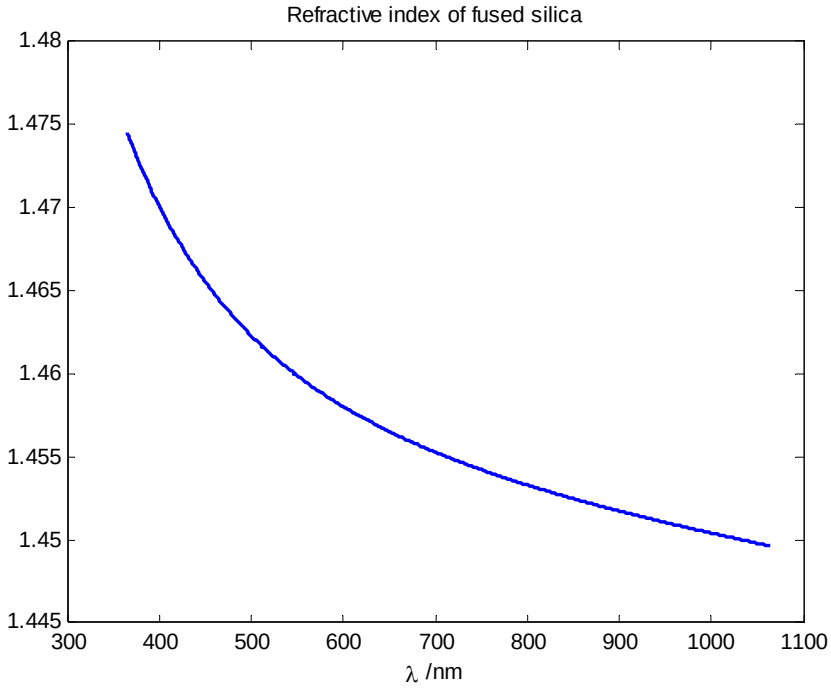

Figure 3.5

The fairly weak birefringence of the material is not taken into account. The differential needed in eq. (1.1) is then given by:

$$\frac{dn}{d\lambda} = \frac{1}{2n(\lambda)}\left(2A_1\lambda - 2A_2\lambda^{-3} - 4A_3\lambda^{-5} - 6A_4\lambda^{-7} - 8A_5\lambda^{-9}\right) \qquad (3.5)$$

SHG and THG crystals

Two materials frequently used for second and third harmonic generation are BBO and KDP. Both these crystals have quite large differences in group velocity between the fundamental and the second harmonic. So the generated harmonic lags behind the pump pulses as the pulses propagate through the crystal.

So for SHG the harmonic lags behind the fundamental. Since more harmonic is generated by the fundamental all the way through the crystal, the harmonic will be broadened to longer pulse duration than the fundamental. The solution is to use a very thin crystal so that the broadening

is small. Typical values are about 0.1 mm. Even if the peak power of the femtosecond lased is very high, the short crystal makes it difficult to efficiently generate harmonics. It is therefore vital to use nonlinear materials with large nonlinear coefficients. Here BBO has a large advantage over KDP. But the difference in group velocities is also larger in BBO meaning that a KDP crystal can be a made a little thicker. However the nonlinear coefficients for BBO are almost 6 times higher than for KDP, so BBO is still the better choice.

Then when generating the third harmonic this is done by mixing the fundamental and second harmonic. This process is possible to phase match in both in KDP and BBO, but due to the low nonlinear coefficients of KDP, only BBO is used. Since the fundamental and second harmonic propagate at different velocities they will only overlap over a limited distance. If they get completely separated they cannot interact and the harmonic generation will stop. Because of this there is no point in using a thick crystal for THG.
The third harmonic also has a group velocity which is a lot slower than both the fundamental and second harmonic. So the third harmonic will have even longer pulse duration than the second harmonic.

The refractive index for the two materials can be described by the Sellmeier relations that give a good approximation of the refractive index as a function of wavelength.

The group velocity for KDP and BBO is given by eq. (1.2). The difference from fused silica lies in the formula for the refractive index. First, the ordinary and extraordinary refractive index is given by the Sellmeier relation. The coefficients can easily be found in most crystal manufacturer's datasheets, and are included in Appendix B.

KDP:

$$n_o^2 = A_o + \frac{B_o \lambda^2}{\lambda^2 - C_o} + \frac{D_o}{\lambda^2 - E_o}$$
$$n_e^2 = A_e + \frac{B_e \lambda^2}{\lambda^2 - C_e} + \frac{D_e}{\lambda^2 - E_e} \qquad (3.6)$$

Here the refractive indices are drawn as a function of wavelength.

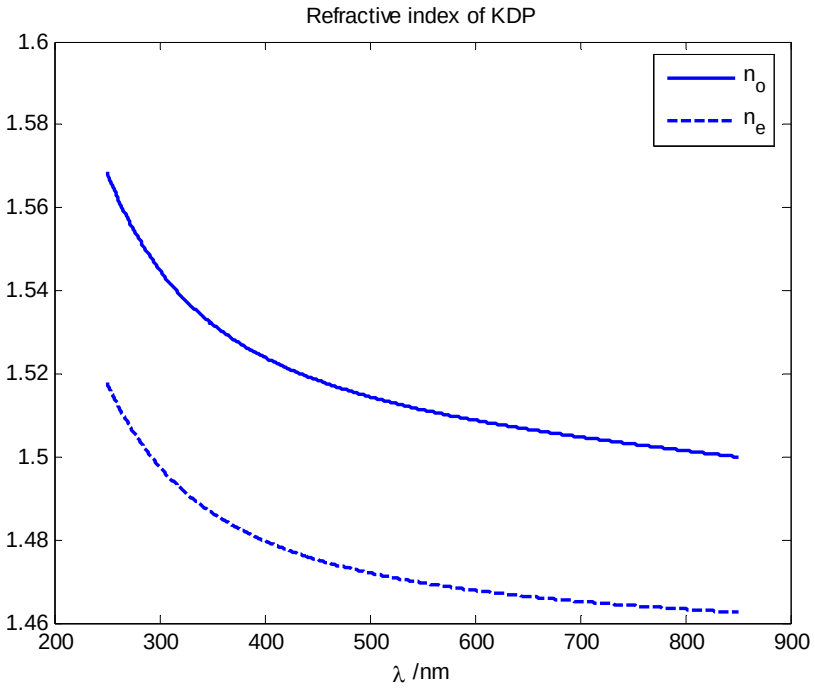

Figure 3.6

The indices *o* and *e* indicates ordinary or extraordinary.
The differentials of these two will be needed:

$$\frac{dn_j}{d\lambda} = -\frac{1}{n_j}\left(\frac{B_j C_j \lambda}{\left(\lambda^2 - C_j\right)^2} + \frac{D_j \lambda}{\left(\lambda^2 - E_o\right)^2}\right) \tag{3.7}$$

Here the index *j* is to be replaced by *o* or *e*.

BBO:

BBO differs from KDP in the form of the Sellmeier relation. The refractive indexes are given by:

$$n_o^2 = A_o + \frac{B_o}{\lambda^2 - C_o} - D_o\lambda^2$$
$$n_e^2 = A_e + \frac{B_e}{\lambda^2 - C_e} - D_e\lambda^2 \qquad (3.8)$$

Refractive indices drawn as a function of wavelength:

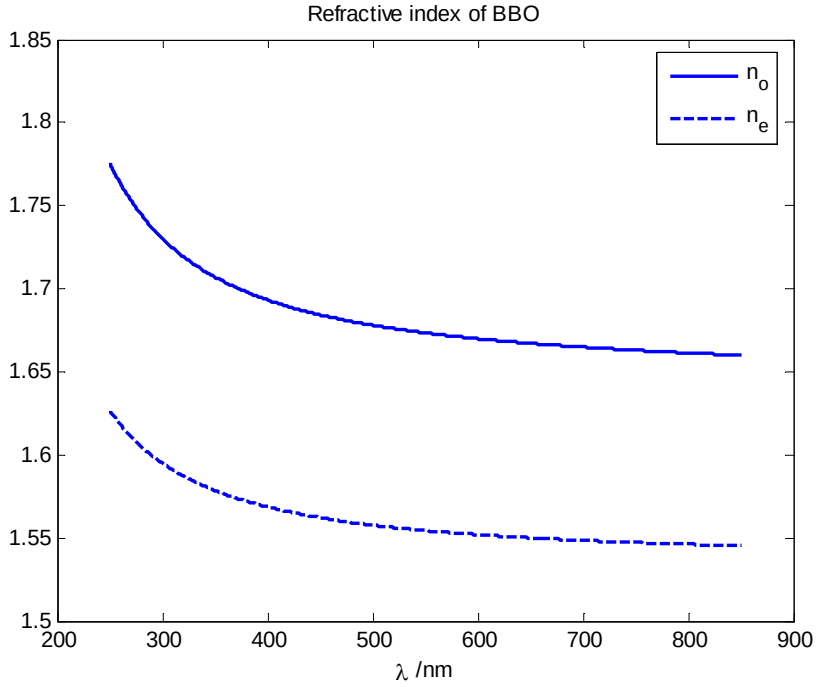

Figure 3.7

With derivatives:

$$\frac{dn_j}{d\lambda} = -\frac{1}{n_j}\left(\frac{B_j\lambda}{\left(\lambda^2 - C_j\right)^2} + 2D_j\lambda\right) \qquad (3.9)$$

Both materials are highly birefringent. Thus the transmitted light is divided into two parts called the ordinary and the extraordinary wave. The ordinary wave behaves like it would in isotropic media. The extraordinary wave however will experience a refractive index that depends on the angle

between the surface normal and the optical axis of the crystal. This is given by the formula for the index ellipsoid:

$$\frac{1}{n(\theta)^2} = \left(\frac{\cos^2\theta}{n_o^2} + \frac{\sin^2\theta}{n_e^2} \right)^{-1} \tag{3.10}$$

When rewritten the refractive index becomes:

$$n(\theta) = \left(n_0^{-2}\cos^2\theta + n_e^{-2}\sin^2\theta \right)^{-1/2} \tag{3.11}$$

The differential is then given by:

$$\frac{dn(\theta)}{d\lambda} = n(\theta)^3 \left(\frac{\cos^2\theta}{n_o^3}\frac{dn_o}{d\lambda} + \frac{\sin^2\theta}{n_e^3}\frac{dn_e}{d\lambda} \right) \tag{3.12}$$

The group velocities for the two waves thus become:

$$\begin{aligned} v_g^o &= v_F^o \left(1 + \frac{\lambda}{n_o}\frac{dn_o}{d\lambda} \right) \\ v_g^e &= v_F^e \left(1 + \frac{\lambda}{n_e}\frac{dn(\theta)}{d\lambda} \right) \end{aligned} \tag{3.13}$$

3.1.3 Correcting the time delay

3.1.3a Delay line

The time delay between the pulses can be corrected with a delay line consisting of beamsplitters and mirrors.

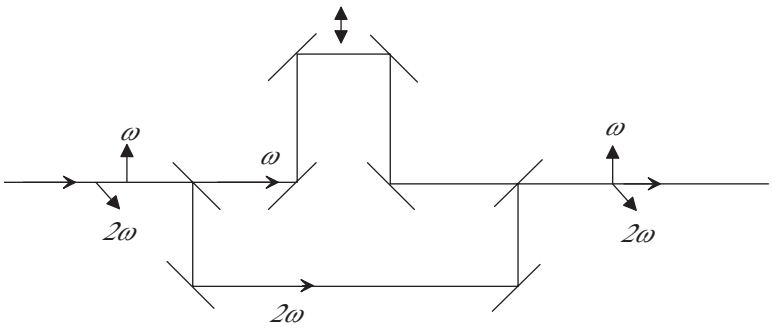

Figure 3.7: A traditional delay line consisting of beamsplitters and mirrors.

This gives the possibility to adjust the path length difference between the fundamental and second harmonic. The main drawback of this design is that the mirrors and beam splitters introduce severe losses. It is also very difficult to align, and once aligned very sensitive. For example, the pulses from a 35 fs laser are about 10 μm long. So for the time delay to be reasonably easy to align, the precision of the translation stage will have to be better than this.

3.1.3b Group velocity compensation plate

An attractive alternative to the delay line is to use a tunable group velocity compensation plate to correct the time delay. This is a birefringent crystal which is cut with the optical axis oriented in a suitable angle. Two suitable materials are BBO and calcite. Both materials have lower refractive index for the extraordinary wave and are thus called *negative uniaxial*.

When using type 1 phase matching the fundamental and second harmonic are polarized perpendicular to each other. If the compensation plate is oriented so that the optical axis is perpendicular to the polarization of the fundamental, the second harmonic will become the extraordinary wave and thus experience a lower refractive index than the fundamental. Then by turning the compensation plate the time delay can be adjusted. The compensation plate has to sit in front of the half wave plate, since it only works because of the different polarizations. Here is a schematic of how this will look.

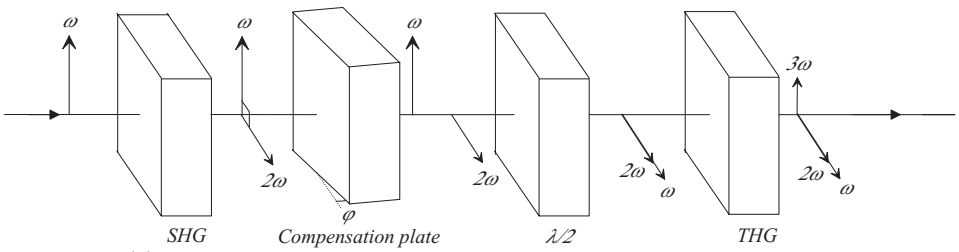

Figure 3.8: THG with half wave plate and group velocity compensation.

The behavior of the extraordinary wave is fairly complex due to the walk off. In negative crystals the extraordinary wave bends way from the optical axis. This is a simple example with normal incidence.

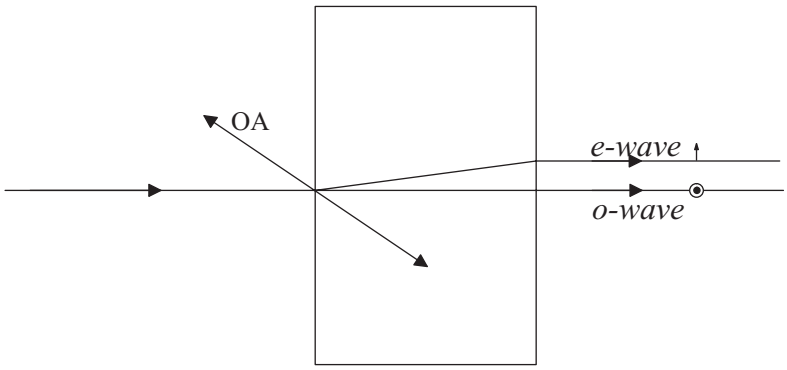

Figure 3.9: Unpolarized beam hits a birefringent material and is divided into two parts.

Usually the energy transport is directed along the *k*-vector, which means that a beam propagates along its *k*-vector. In birefringent materials the energy in the extraordinary wave is shifted sideways by the birefringence, so that the beam no longer propagates along the *k*-vector. The *k*-vector is still however perpendicular to the wave fronts. This is illustrated below.

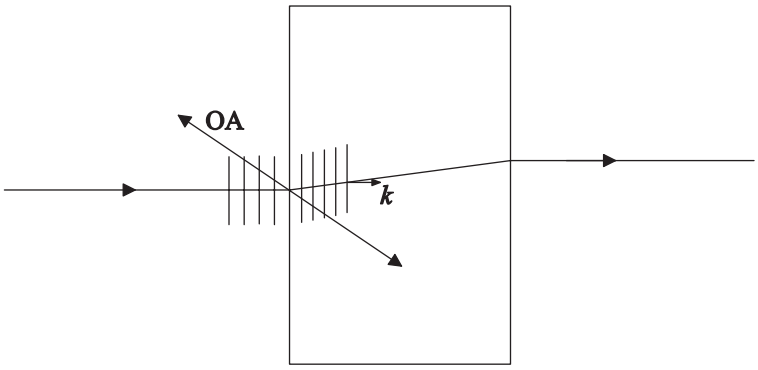

Figure 3.10: The wave fronts and the *k*-vector for the e-wave.

In this simple case of normal incidence the time delay can be calculated just by using the index ellipsoid. However when the incidence of the light is not normal, a more complex approach is needed. One method is to solve Maxwell's equations. This is done in reference [2]. and the result is discussed below.

Depending on the angle of incidence and the orientation of the optical axis, the extraordinary wave can propagate in a direction closer to, or further away from the surface normal than the ordinary wave. When the direction is closer to the normal the path through the crystal for the extraordinary wave becomes shorter. This is one part of the behavior when the compensation plate is turned. The other effect is that the refractive index for the extraordinary wave changes with the angle of incidence.

As illustrated below, θ is the angle between the surface normal and the optical axis, and φ is the angle of incidence, called tuning angle.

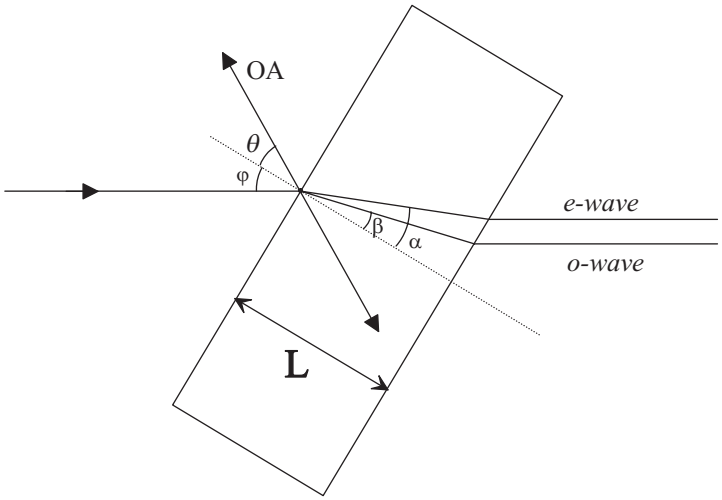

Figure 3.11: Illustration showing how the angles are defined.

The solution for the extraordinary wave direction given in reference [2] is more complex than needed. For this application it can be simplified considerably. It is assumed that the crystals are surrounded by air, and that $n_{air} = 1$.
The direction of propagation for the extraordinary wave is then given by:

$$\tan\alpha = \frac{Q_e \sin\theta\sin\varphi - \left(\varepsilon_o - Q_e^2\right)\cos\theta}{Q_o^2 \sin\theta - Q_e \sin\theta\sin\varphi} \tag{3.14}$$

And the direction of the extraordinary wave's *k*-vector is given by:

$$\tan\alpha_k = \frac{\sin\varphi}{\mathrm{Q_e}} \tag{3.15}$$

It is worth to notice that if $\Delta\varepsilon$ is set to zero, which would mean that the material is not birefringent, the expression (3.14) collapses into (3.15).

The constants here are defined:

$$D = \left[\varepsilon_o\varepsilon_e\left(\varepsilon_o + \Delta\varepsilon\cos^2\theta - \sin^2\varphi\right)\right]^{1/2} \tag{3.16}$$

$$Q_o^2 = \varepsilon_o - \sin^2\varphi \tag{3.17}$$

$$Q_e = \left(D - \frac{\Delta\varepsilon}{2} \sin 2\theta \sin\varphi \right) \Big/ \left(\varepsilon_o + \Delta\varepsilon \cos^2\theta \right) \tag{3.18}$$

Then the direction of propagation is calculated for the ordinary wave:

$$\sin\beta = \frac{\sin\varphi}{n_o} \tag{3.19}$$

In figure 3.10 the wave propagation in a birefringent material is shown. The index ellipsoid gives the index of refraction for the direction of the *k*-vector. The beam however generally propagates in a slightly different direction. But it is the distance between the wave fronts along the k-vector that determines the propagation velocity. So in order to determine the propagation velocity it is the *k*-vector that should be considered.

By using eq (1.10) with the angles defined above the index of refraction for the *k*-vector thus becomes:

$$n_k = \left(n_0^{-2} \cos^2\left(\alpha_k + \theta\right) + n_e^{-2} \sin^2\left(\alpha_k + \theta\right) \right)^{-1/2} \tag{3.20}$$

And the differential:

$$\frac{dn_k}{d\lambda_2} = n_k^3 \left(\frac{\cos^2\left(\alpha_k + \theta\right)}{n_o^3} \frac{dn_o}{d\lambda_2} + \frac{\sin^2\left(\alpha_k + \theta\right)}{n_e^3} \frac{dn_e}{d\lambda_2} \right) \tag{3.21}$$

If we now take a look at the beam paths through the crystal, we can derive expressions for the different path lengths from the geometry.

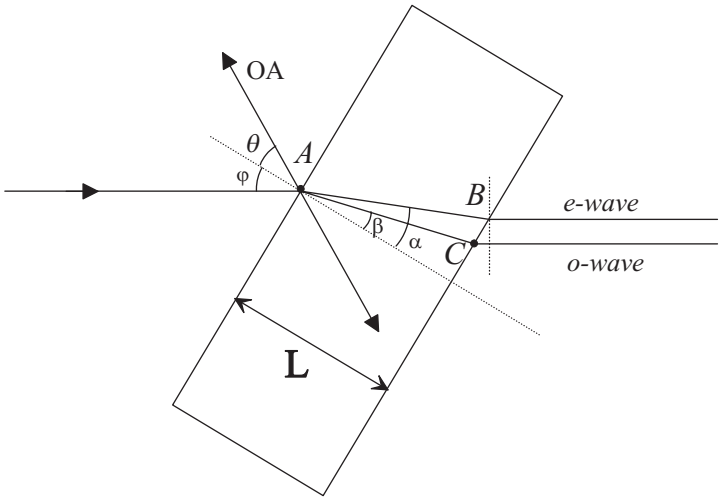

Figure 3.12: Illustration of the different paths through the crystal.

The two waves separate at point A. And then from the cross section B they propagate parallel to each other again with a small offset. In the real setup this offset is much smaller than the beam diameter and which means it will not affect the result. To get to cross section B the ordinary wave passes through the crystal, AC, and then through air, CB.
The e-wave only passes through the crystal, AB.
Starting with the o-wave. The distance AC is given by:

$$AC = \frac{L}{\cos\beta} \tag{3.22}$$

Then the distance CB is:

$$CB = L\left(\tan\alpha - \tan\beta\right)\sin\varphi \tag{3.23}$$

Then for the e-wave, the distance AB is not the true path length since the *k*-vector is in another direction. The effective distance is instead given by the projection of AB onto the *k*-vector.

$$AB_{eff} = \frac{L}{\cos\alpha}\cos\left(\alpha - \alpha_k\right) \tag{3.24}$$

Then the group velocities are calculated using eq (1.2)

$$v_g^o = v_F^o\left(1+\frac{\lambda}{n_o}\frac{dn_o}{d\lambda}\right)$$
$$v_g^e = v_F^e\left(1+\frac{\lambda}{n_k}\frac{dn_k}{d\lambda}\right) \qquad (3.25)$$

The time delay can then be calculated:

$$\Delta t = t_o - t_e = \underbrace{\frac{AC}{v_g^o}+\frac{CB}{c}}_{\text{o-wave}} - \underbrace{\frac{AB_{eff}}{v_g^e}}_{\text{e-wave}} \qquad (3.26)$$

With this definition of the time delay a positive value means that the extraordinary wave passes faster. If the time delay as a function of tuning angle is drawn in a diagram the result can look like this. The curve is drawn by the MatLab program found in Appendix A.

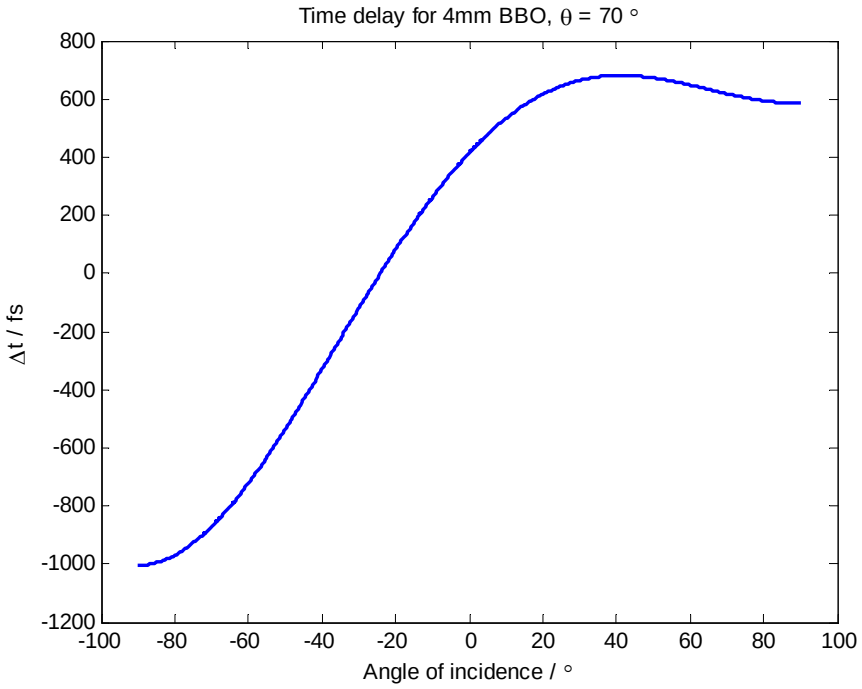

Figure 3.13: Example curve for a BBO compensation plate.

Here BBO is used, but the compensation plate may be made of any strongly birefringent material. One possible choice is Calcite. It has the same formulation of the Sellmeier relation as BBO, only with other values for the coefficients. Therefore the exact same formulas can be used. Compared to BBO, Calcite has larger birefringence, which means that a Calcite compensation plate will have a larger tuning range. But the damage threshold is lower than for BBO, and the surface quality can not be made as good. Here is an example curve for a Calcite compensation plate.

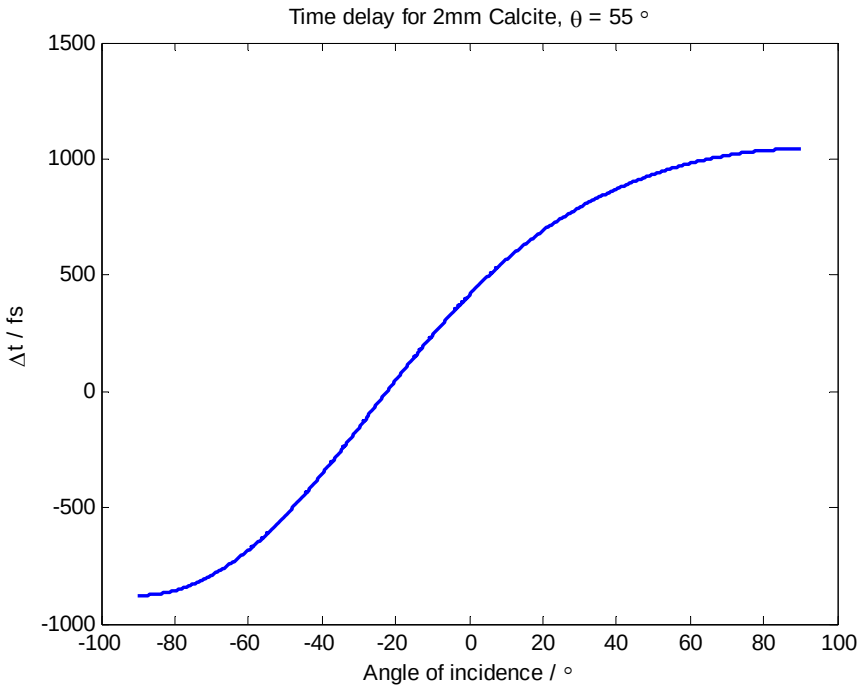

Figure 3.14: Example curve for a Calcite compensation plate.

Because of the larger birefringence the 2 mm Calcite compensation plate gives roughly the same tuning range as a 4 mm BBO. So when the damage threshold and surface smoothness are not a concern Calcite might be an interesting alternative.

3.2 Single crystal THG

The third harmonic can also be produced by a one step process in a single crystal. That means that only one optical component is required, which makes for a very simple setup.
The third harmonic generation is then dependant on the third order term in the nonlinear polarization. The process is possible in several materials, for instance both BBO and KDP can be used. Unfortunately the third order susceptibility is very weak The crystal therefore has to be thick, and due to the group velocity difference the generated third harmonic pulses then become much longer than the fundamental.
This approach was never tested in the lab because no suitable crystal was available.

3.3 Focusing in air

Focusing in air is the easiest way to produce the third harmonic with high peak power lasers. The setup is simple and inexpensive since only standard optics is needed. Gases generally have very low nonlinear susceptibility, which means that the intensity has to be very high in order for the nonlinear effects to be noticeable. Because of the centrosymmetric nature of gases all the even order terms in the expansion of the nonlinear polarization is zero. Therefore only the odd harmonics are produced. And of these the third harmonic normally is dominant. By focusing the beam for instance with a lens the peak intensity in the beam waist can get extremely high. The peak intensity obviously depends on the diameter of the beam waist, which for a beam of diameter D and a lens of focal length f is given by:

$$2w_0 = \frac{4\lambda f}{\pi D} \tag{3.27}$$

The peak intensity thus gets higher with a shorter focal length. But at the same time the focal region with high intensity becomes shorter. And if the intensity becomes too high there will be white light generation, which means that a broad continuum of wavelengths is produced instead.

Phase matching is not a problem since the refractive index of air remains close to 1 for the different wavelengths. That also means that the group velocity for the fundamental and the third harmonic are almost the same, so

that the harmonic will not be broadened by group velocity mismatch. The weak nonlinear properties of air combined with the short interaction length means that the conversion efficiency is low.

If the beam is focused into a capillary tube the interaction length can be greatly increased. The tube will then keep the beam focused for a long distance. But then the phase matching can be lost. This is solved by putting the tube into a vacuum chamber in which the pressure can be varied. The pressure is then adjusted until phase matching is achieved. The conversion efficiency can also be increased by using other gases such as argon. The advantages of this method are that very short pulses can be produced with good conversion efficiency, but the needed setup is large and fairly complex since a vacuum chamber is needed. For details see [4].

4 Experimental work

The experiments were done in the laser hutch at MaxLab beamline D611. The laser consists of a Ti:sapphire oscillator and a Ti:sapphire chirped pulse amplifier. The oscillator is synchronized to the MaxII bunch clock to allow pump-probe experiments to be done with precision timing.
The amplifier has a high repetition rate which is currently set to 5 kHz.
The standard output power when the amplifier is perfectly aligned is about 5 W which then translates to 1mJ per pulse. The optimal pulse duration is ~30 fs. During the work on this Master Thesis the output power was around 3.6 W, meaning that the alignment was not perfect. It is unknown if and how the pulse duration was affected.
The laser output is divided into several beams, and the maximum power available in the beam used was around 2 W.

4.1 Group velocity compensation plate.

To test the effectiveness of the group velocity compensation plate a setup was built after figure 3.8. The crystals used initially were:

SHG:
KDP, θ=29.2°, 0.25 mm

Group velocity compensation plate:

Calcite, θ=25°, 2.0 mm

THG:
BBO, θ=45°, 0.05 mm

The half wave plate was made of quartz, 2 mm thick.
A prism was used to separate the individual harmonics and the fundamental.
The telescope consists of one positive and one negative lens, with tube length $f_1 + f_2$. This was put in to downsize the beam diameter to make the peak intensity higher. Another advantage is that smaller and thus cheaper crystals could be used.

The third harmonic power was measured with a standard photo diode. Photo diodes are usually mounted in a metal housing with a glass window. This window will not transmit UV light, but if this protective glass is removed the bare diode will work very well in the UV range. The downside of the diode is that it is not at all calibrated, so it is unknown how linear it is, and what power a given diode current corresponds to. However at the low currents measured here it should be very linear. The current is also largely dependent on where the beam hits, the edges of the diode seemed to be more sensitive than the central region. In some measurements a piece of thin paper was put in front of the diode as a diffuser to reduce this problem.
A Molectron PowerMax power meter was also used. This detector has a resolution of approximately 1 mW.

A top view schematic of the setup:

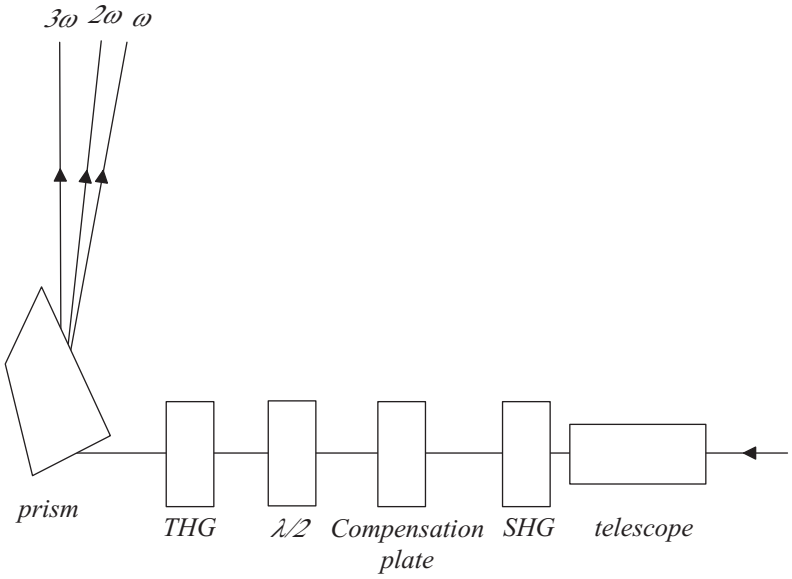

Figure 4.1: Schematic view of the experimental setup.

Here is a photograph of the setup.

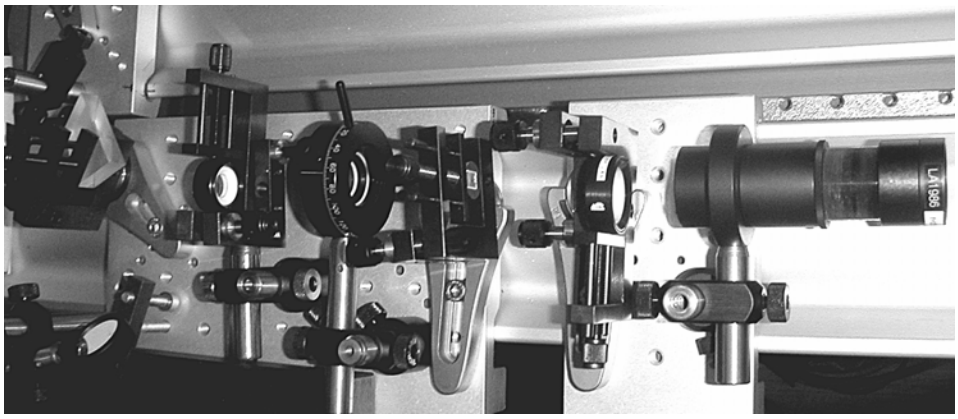

Picture 4.1: Photograph of the experimental setup.

For the given optics the time delay between the fundamental and second harmonic from the half wave plate is 341 fs. The delay from the second harmonic crystal is 35 fs.
It is also a good idea to pre-compensate for part of the delay between the fundamental and the second harmonic in the third harmonic crystal. This

gives the two pulses a longer distance to interact which will improve conversion. The delay in this case is 18 fs.
This then gives a total delay of approximately 380 fs to be corrected.
The compensation plate used has this time delay curve:

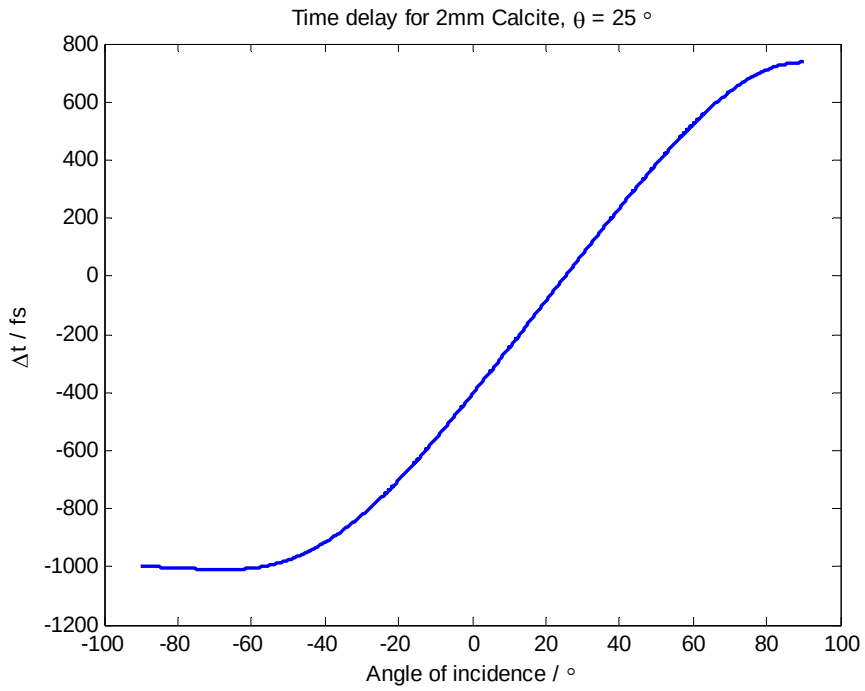

Figure 4.2

The desired time delay of 380 fs is found at a tuning angle of almost 50 degrees. When the setup was fully optimized the tuning angle ended up being slightly larger than this. This discrepancy is probably mainly because of the use of parameters for fused silica instead of quartz for the half wave plate.

At this large angle of incidence the reflections from the compensation plate surface were quite large for the fundamental, which is s-polarized to this surface. This loss limited the efficiency of the third harmonic generation. The output power was too low to be measurable by the PowerMax power meter.

To improve the setup the Calcite compensation plate was replaced by a borrowed one made of BBO with thickness 6mm, and θ=65°.

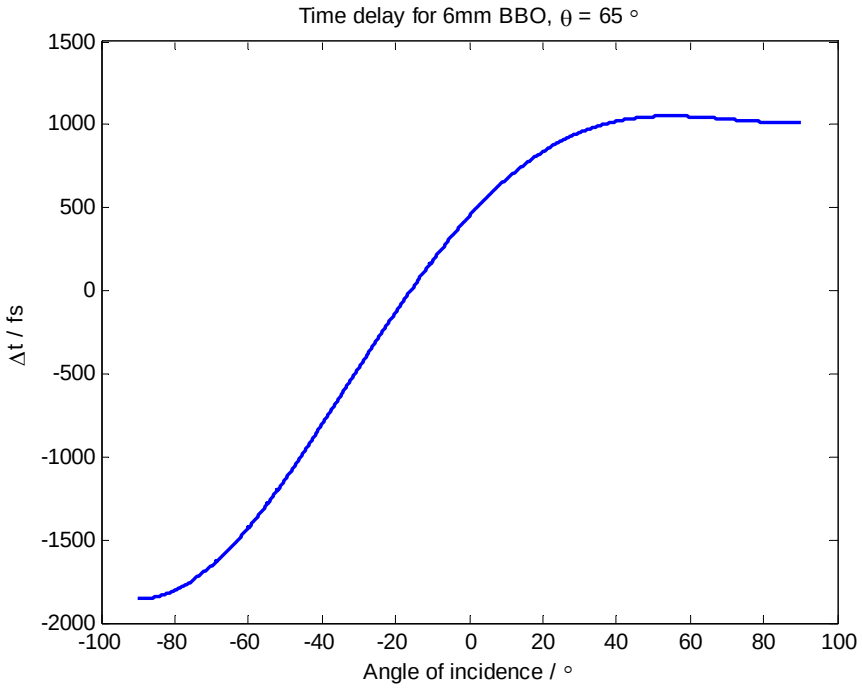

Figure 4.3

This crystal has a tuning curve with is better suited to the setup. The desired delay of about 380 fs is reached almost at normal incidence, and with a fairly linear behavior around that angle.
And the second harmonic generation crystal was changed to one made of BBO, with thickness 0.25 mm, and θ=29.2°.
These changes boosted the third harmonic power considerably.

A few measurement series was done to investigate the third harmonic power when the pump power, the second harmonic power and the tuning angle was varied.

4.2 Air

The third harmonic generation in air was not expected to give very efficient conversion. But the simple and inexpensive setup still makes it an interesting alternative. Therefore a setup was built to test the method.
In these experiments the laser was simply focused in air with a BK7 plano-convex lens. Then a fused silica lens was used to recollimate the beam

before harmonic separation. Here a BK7 glass lens would not have worked since it is not transparent to the third harmonic. The harmonic separator consisted of the same prism as before. The third harmonic was then measured with the photo diode. Unfortunately the power was too low to be reliably measured by the Moltectron PowerMax power meter.
The focusing lens that gave the best result was one with f=150 mm. The short focal length made it troublesome to recollimate the light as only one fused silica lens was available, with f=300 mm. This meant that it was not possible to make the beam parallel again as it would then have too large a diameter to pass the harmonic separating prism. The solution was to instead make the beam convergent, so that it would pass the prism unhindered. One advantage of this was that the beam diameter on the photo diode was small enough so that the entire beam could hit the sensitive area. It would have been interesting to try focusing lenses with even shorter focal lengths, but then it would not have been possible to collect all the generated harmonic with the one available fused silica lens.

The third harmonic power was then measured with the photo diode at various input powers.

5 Results from the experiments

5.1 Group velocity compensation plate.

The measurements were done mainly to determine how the conversion efficiency depends on different parameters. The parameters that can be easily changed are IR power, second harmonic power and tuning angle. The second harmonic power can be varied by turning the SHG crystal slightly out of alignment, meaning that the phase matching will not be perfectly fulfilled.

First, the third harmonic power as a function of tuning angle

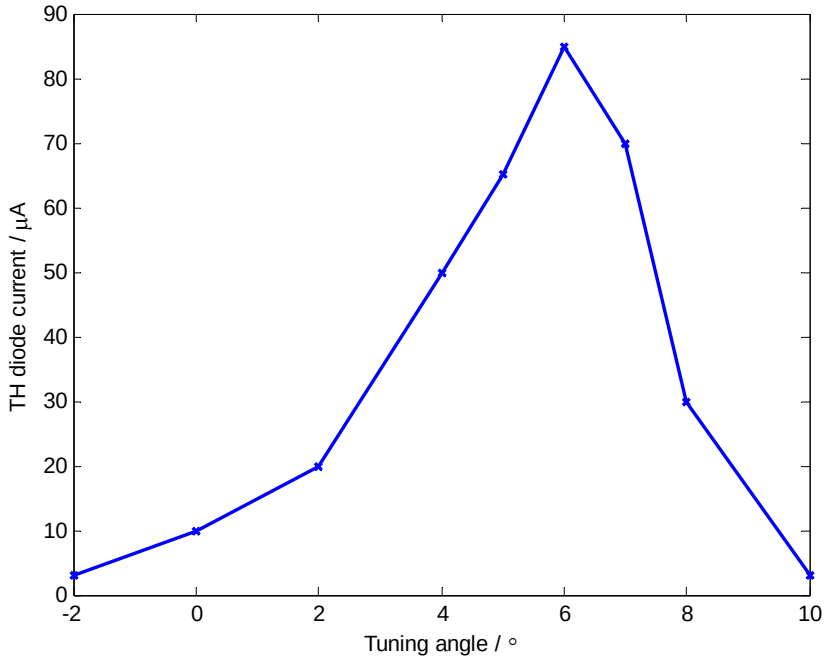

Figure 5.1: The third harmonic diode current as a function of tuning angle.

There is a clear peak at approximately 6 degrees, but it is surrounded by a fairly wide region where the setup produces some third harmonic. Because of this the time delay was very easy to align.

Then, the third harmonic power as a function of IR power. Both the third and second harmonic power was measured while the input IR power was varied. The second harmonic power is lower than it should be since it was measured after some of it had been converted to third harmonic.
Both the second and third harmonic powers show a clear quadratic behavior, which was verified by plotting them in a log-log diagram.
The maximum third harmonic power was around 8 mW.

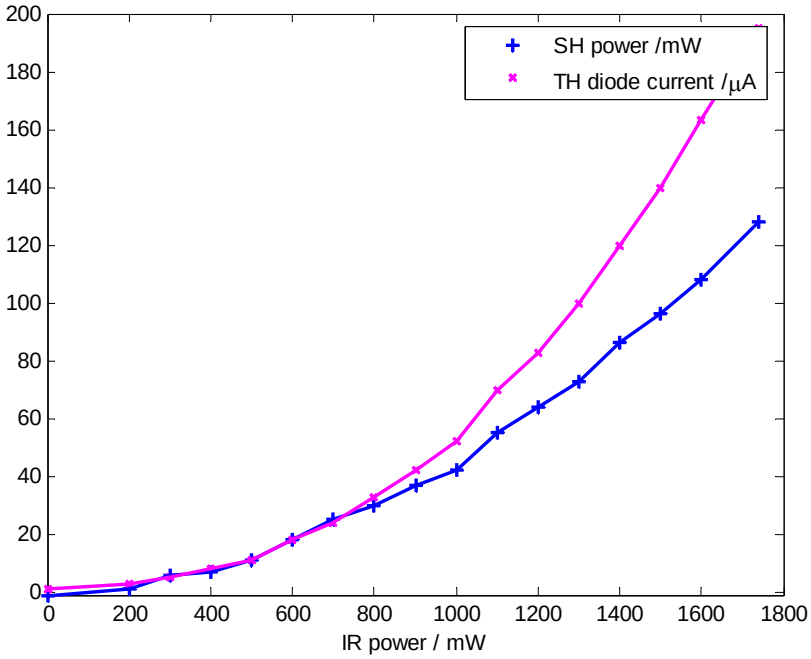

Figure 5.2: Second and third harmonic as functions of IR power.

In the last measurement series the input IR power was held constant, and the SHG-crystal was turned out of alignment to adjust the second harmonic power. Also here the second harmonic power was measured after third harmonic generation, so the value is not entirely true. But the second harmonic power was so much greater than the third harmonic, that the error should be minor.

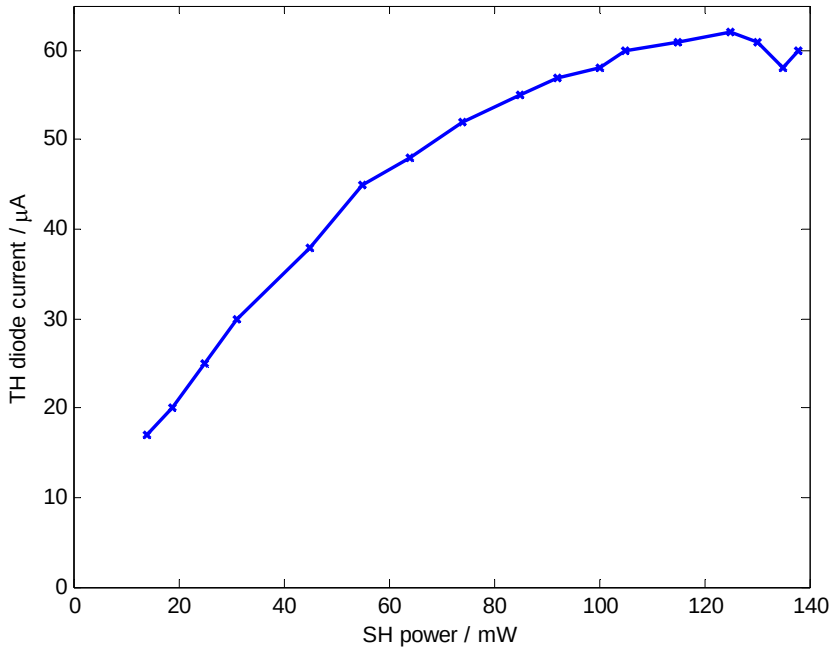

Figure 5.3: Third harmonic diode current measured as a function of SHG conversion efficiency.

In the last figure it can be seen that the third harmonic power does not depend very strongly on the second harmonic generation efficiency.

5.2 Air

The third harmonic power from this experiment could not be measured with the PowerMax meter since the power was below the 1 mW resolution limit of the detector. So only the photo diode was used.

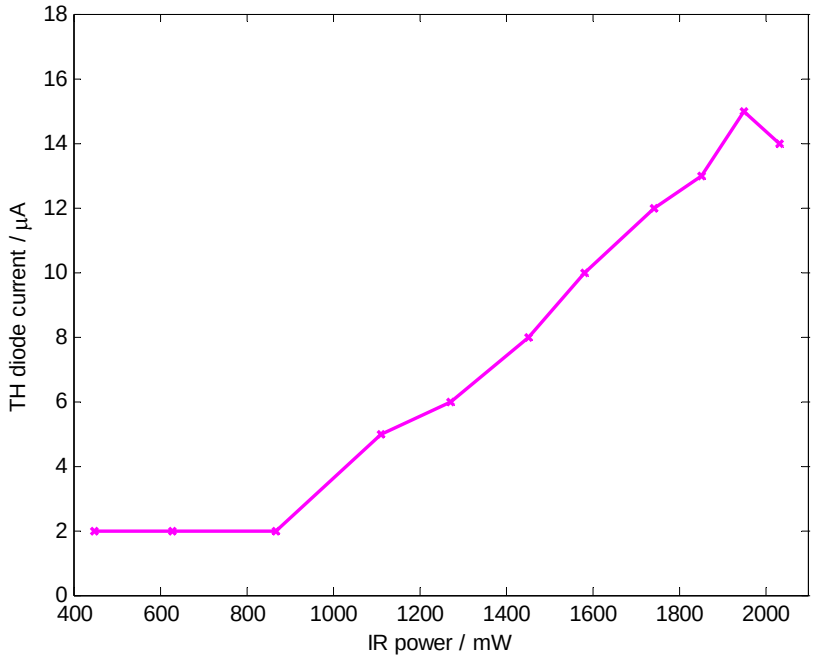

Figure 5.4: Third harmonic diode current as a function of IR power.

Here it is evident that this method is very inefficient. A measurable signal was not produced until the input power reached ~1 W. Surprisingly the third harmonic power seems to depend linearly on the input power. But the uncertainties in the measurements were quite large, especially at the lower input powers.

6 The permanent setup

From the experiments it was decided to build the permanent setup using the group velocity compensation plate. The available space in the lab was very limited so a more compact version had to be built. This was accomplished by using compact optical mounts on a small breadboard.
Here is a photograph of the finished tripler.

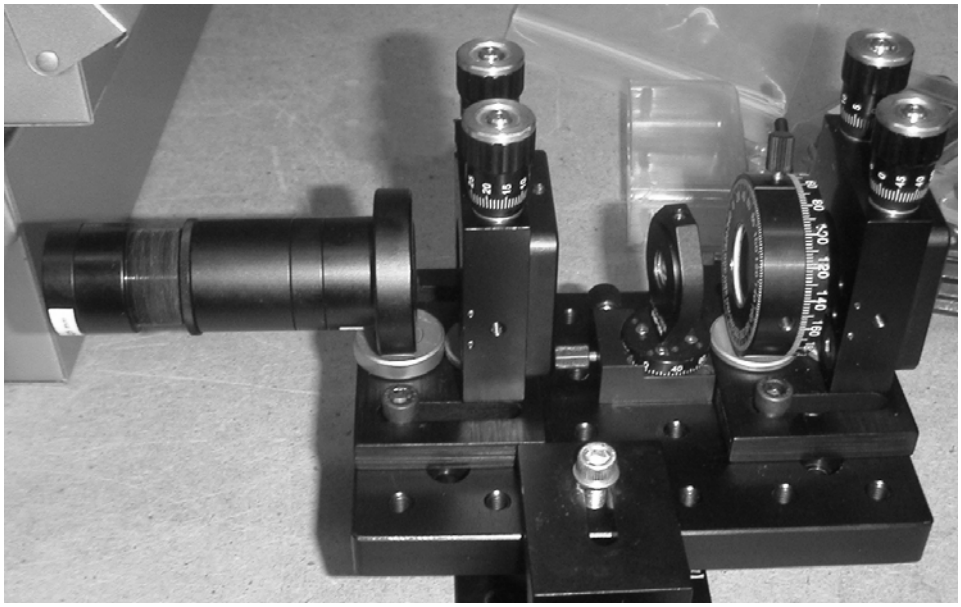

Picture 6.1: Photograph of the finished tripler.

When this is being written the new crystals for the permanent setup have not yet arrived. The final configuration will be:

SHG:
BBO, θ=29.2°, 0.2 mm

Group velocity compensation plate:
BBO, θ=70°, 4.0 mm

THG:
BBO, θ=45°, 0.1 mm

The tuning curve for this compensation plate is shown as an example in figure 3.1.3.

7 Summary

The goal of this Master Thesis has been to construct a compact and efficient frequency tripler for a Ti:sapphire laser. Two possible solutions have been investigated. These were THG in air, and a nonlinear crystal-based setup using a group velocity compensation plate. The conversion in air did not provide enough conversion efficiency. But the setup using the compensation plate worked very well and provided good conversion efficiency, while still being easy to align.. Therefore the final setup has been built using the compensation plate. This is now installed at MaxLab beamline D611.
A MatLab program has been written to show the time delay as a function of tuning angle for a given crystal when used as a group velocity compensation plate. The program can be found in Appendix A.

This report and the MatLab program are also available on the internet:
http://www-atom.fysik.lth.se/txrd/henrikexjobb.pdf
http://www-atom.fysik.lth.se/txrd/henrikexjobbprog.m

8 Acknowledgments

First I would like to thank my supervisor Prof. Jörgen Larsson for giving me the opportunity to do this exciting project as a Master Thesis.

Then I would like to thank Dr. Tue Normann Hansen for all the help with the experiments, and for starting and stopping the laser system for me.

I would also like to thank Dr. Alok Srivastava for ideas and suggestions on this report, and for being a great room-mate.

And thank you Michael Harbst and Ola Synnergren for all the encouragement along the way.

9 References

[1] **Larsson, J.** Laser and synchrotron radiation pump-probe x-ray diffraction experiments, Meas. Sci. Technol. **12** (2001) 1835 – 1840

[2] **Lekner, J.** Reflection and refraction by uniaxial crystals, *J Phys: Condes Matter*, **3** (1991) 6121 – 6133

[3] **Banks, P. S. Feit, M. D. Perry, M. D.** High-intensity third-harmonic generation, *J. Opt. Soc. Am. B,* **19** (2001) 102 – 118

[4] **Backus, S. Peatross, J. Zeek, Z. Rundquist, A. Taft, G. Murnane, M. M. Kapteyn, H. C.** 16-fs, 1μJ ultraviolet pulses generated by third-harmonic conversion in air, *Opt. Lett.,* **21** (1996) 665 – 667

[5] **Yariv, A. Yeh, P.** Optical waves in crystals, Wiley (1984)

[6] **Pedrotti, F. L. Pedtrotti, L. S.** Introduction to Optics, second edition, Prentice Hall (1996)

[7] **Morgan, J.** Geometrical and physical optics, McGraw-Hill (1953)

[8] **Boyd, R.W.** Nonlinear Optics, Academic Press (2003)

Appendix A: comp_plate.m

This source code is also available on the internet:
http://www-atom.fysik.lth.se/txrd/henrikexjobbprog.m

```
%Fundamental wavelength
lambda1=780e-9;

%Crystal thickness
L=4e-3;

%Crystal cut-angle
thetadeg=70;

%Crystal material, valid are 'BBO' and 'Calcite'
ctype='BBO';


lambda2=lambda1/2;
c=3e8;
theta=thetadeg*pi/180;

%Sellmeier
if strcmp(ctype, 'BBO')
    %Coefficients for BBO
    Ao=2.7405;
    Bo=0.0184e-12;
    Co=0.0179e-12;
    Do=0.0155e12;
    Ae=2.3730;
    Be=0.0128e-12;
    Ce=0.0156e-12;
    De=0.0044e12;
end

if strcmp(ctype, 'Calcite')
    %Coefficients for Calcite
    Ao=2.69705;
    Bo=0.0192064e-12;
    Co=0.01820e-12;
```

```
    Do=0.0151624e12;
    Ae=2.18438;
    Be=0.0087309e-12;
    Ce=0.01018e-12;
    De=0.0024411e12;
end


% 2:nd harmonic is the extraordinary wave
epso=Ao + Bo/(lambda2^2-Co) - Do*lambda2^2;
n2o=sqrt(epso);
epse=Ae + Be/(lambda2^2-Ce) - De*lambda2^2;
n2e=sqrt(epse);

dn2odlambda2 = (1/n2o) * (-Bo*lambda2/(lambda2^2-
Co)^2 - Do*lambda2);
dn2edlambda2 = (1/n2e) * (-Be*lambda2/(lambda2^2-
Ce)^2 - De*lambda2);


% fundamental is the ordinary wave
eps1=Ao + Bo/(lambda1^2-Co) - Do*lambda1^2;
n1=sqrt(eps1);
dn1dlambda1 = (1/n1) * (-Bo*lambda1/(lambda1^2-
Co)^2 - Do*lambda1);

deltaeps = epse-epso;



%vector of tuning angles
fi=linspace(-pi/2,pi/2,600);



D=sqrt(epso*epse*(epso+deltaeps.*(cos(theta).^2)-
sin(fi).^2));

Q2=epso-sin(fi).^2;
```

```
Qe=(D-0.5*deltaeps*sin(2*theta).*sin(fi)) ./
(epso+deltaeps*cos(theta).^2);

AxAz= (Qe.*sin(theta).*sin(fi)-(epso-
Qe.^2).*cos(theta)) ./ (Q2.*sin(theta)-
Qe.*sin(fi).*cos(theta));

%Extraordinary wave propagation angle
alfa=atan(AxAz);

%Extraordinary wave k-vector angle
alfa_k = atan(sin(fi)./ Qe);

%Ordinary wave propagation angle
beta=asin(sin(fi)/n1);


% Refractive index in the direction of the k-
vector
n_alfa_k=1./sqrt(cos(alfa_k+theta).^2./epso+sin(a
lfa_k+theta).^2/epse);
dn_alfa_k = n_alfa_k.^3 .*
(dn2odlambda2.*(cos(alfa_k+theta).^2 ./ n2o.^3) +
dn2edlambda2.*(sin(alfa_k+theta).^2 ./ n2e.^3));


%Path for the ordinary wave
L1_kristall = L./cos(beta);
L1_luft = L*(tan(alfa)-tan(beta)).*sin(fi);



%Path for extraordinary wave projected on the k-
vector
L2= L./cos(alfa).* cos(alfa-alfa_k);


%Group velocities for fundamental and harmonic
Vg1=c/n1 * (1 + lambda1/n1 .* dn1dlambda1);
Vg2=c./n_alfa_k .* (1 + lambda2./n_alfa_k .*
dn_alfa_k);
```

```
%Timedelay
tdelay=( L1_kristall./Vg1 + L1_luft./c -
L2./Vg2)*1e15;

figure(20)
plot(180/pi*fi,tdelay)
xlabel('Angle of incidence / \circ')
ylabel('\Deltat / fs')
title(['Time delay for ' num2str(L*1000) 'mm '
ctype ', \theta = ' num2str(thetadeg) ' \circ'])
grid
```

Appendix B: Coefficients for the materials

All the coefficients given here are valid for wavelengths given in μm.

BBO

	n_o	n_e
A	2.7405	2.3730
B	0.0184	0.0128
C	0.0179	0.0156
D	0.0155	0.0044

Calcite

	n_o	n_e
A	2.7405	2.3730
B	0.0184	0.0128
C	0.0179	0.0156
D	0.0155	0.0044

KDP

	n_o	n_e
A	2.259276	2.132668
B	13.00522	2.2470
C	400	400
D	0.01008956	0.008637494
E	0.012942625	0.012281043

Fused silica

A_0	2.1026513
A_1	-8.5943075E-3
A_2	9.8576238E-3
A_3	-2.4538022E-4
A_4	4.4589827E-5
A_5	-1.9692608E-6